

MULTI-LAYER TEMPORAL NETWORK MODEL OF THE SPACE ENVIRONMENT

Yirui Wang*, Callum Wilson[†] and Massimiliano Vasile[‡]

To investigate the resilience and sustainability of the global space environment, a Multi-layer Temporal Network Model (MTN) is proposed in this paper. The idea of the network model is to study the relationships among groups of objects in space by studying the topology and dynamics of an equivalent network where each node is a group of objects and the link is modelling the relationship. “Multi-layer” indicates different functionalities among the space objects, such as the physics and information, etc. Currently, only physical layer of MTN is considered. By comparing with the simulation results from existing space environment model, the correctness of the network model is first verified. Some experiments are performed to demonstrate the basic functionalities of the proposed MTN.

INTRODUCTION

The space industry is one of today’s most growing sectors, and as a consequence, the number of resident space objects is continuously rising. The growth rate of collisional debris would exceed the natural decay rate in ≈ 50 years.^{1,2} Moreover, when the number of objects increases, chain effects of collision may be triggered, which is known as Kessler Syndrome.³ The Kessler Syndrome refers to a scenario in which earth orbits inevitably become so polluted with satellite-related orbital debris that a self-reinforcing collisional cascade, which destroys satellites in orbit and makes orbital space unusable, is inevitable.⁴ It is therefore essential to develop the necessary techniques to model, understand and predict the current space environment and its future evolution.⁵

There are many existing efforts to model the long-term evolution of the space environment. Space agencies have developed their own models, such as the NASA LEGEND environment model⁶ and ESA’s DELTA model.⁷ Both of these examples have high-fidelity propagators that apply perturbations to all objects in the simulation. Their approaches to modelling collision rates calculate probabilities of collisions within control volumes, which is based on the widely used CUBE method.⁸ This method is also used in MEDEE, developed by CNES,⁹ and SOLEM, developed by CNSA.¹⁰ This approach to modelling environment evolution can be computationally expensive as it often requires propagating each individual object.

Other environment models use some simplifying assumptions to reduce their computational requirement. It is common to divide the environment into discrete bins based on orbital parameters and define the evolution based on the statistics of each bin. One earlier example is IDES, which divides objects into bins based on some spatial and physical parameters.¹¹ INDEMN makes a further

*Title, department, affiliation, postal address.

[†]Title, department, affiliation, postal address.

[‡]Title, department, affiliation, postal address.

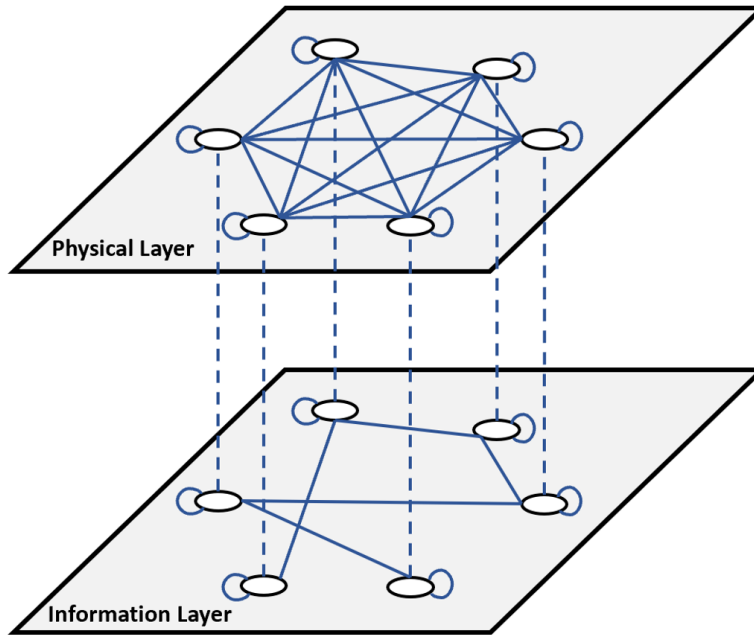


Figure 1: Illustration of the Multi-Layer Temporal Network Model.

simplification of only considering densities of objects in discrete orbital shells in terms of altitude.¹² These approaches allow the generation of much faster estimates of the space environment evolution.

Large constellation is an important factor that affects the evolution of the space debris environment.¹³ Untracked debris will lead to potentially dangerous on-orbit collisions on a regular basis due to the large number of satellites within mega-constellation orbital shells.¹⁴ However, in reality, administrator only has limited resources to focus on certain key nodes in the whole network. Following two questions might be interested: 1) Which nodes should be focused first given limited resources? 2) How much can the network be restored? Several graph theory tools, such as centrality measures¹⁵ and percolation theory,¹⁶ can be used for studying the topology of the network, therefore, the importance of the node and the resilience of the network system can be characterized.

This paper proposes a Multi-layer Temporal Network Model (MTN) to study the relationships among space objects and the spread of catastrophic events, where each node indicates a group of space objects that share common properties, and each link indicates their interaction. The interactions can take the form of physical collisions or cyberattacks. The relationships among the nodes are time-dependent, which allows us to capture the complex dynamics of the space environment. Rather than studying individual aspects of the space environment in isolation, the 'multi-layer' structure connects each aspect to others. Figure 1 shows the illustration of a two-layer MTN, which includes a physical layer and an information layer. Currently, the physical layer of the network model is studied. In Section 2, we discuss the dynamics of the chosen network. Then, in Section 3, we characterize the properties of the network model based on graph theoretical tools. Whereas in Section 4, we present some test cases, where we study the resilience, dynamics, and stability of the space environment through the network theory. Finally, in Section 5, we conclude with some remarks and recommendations for future work.

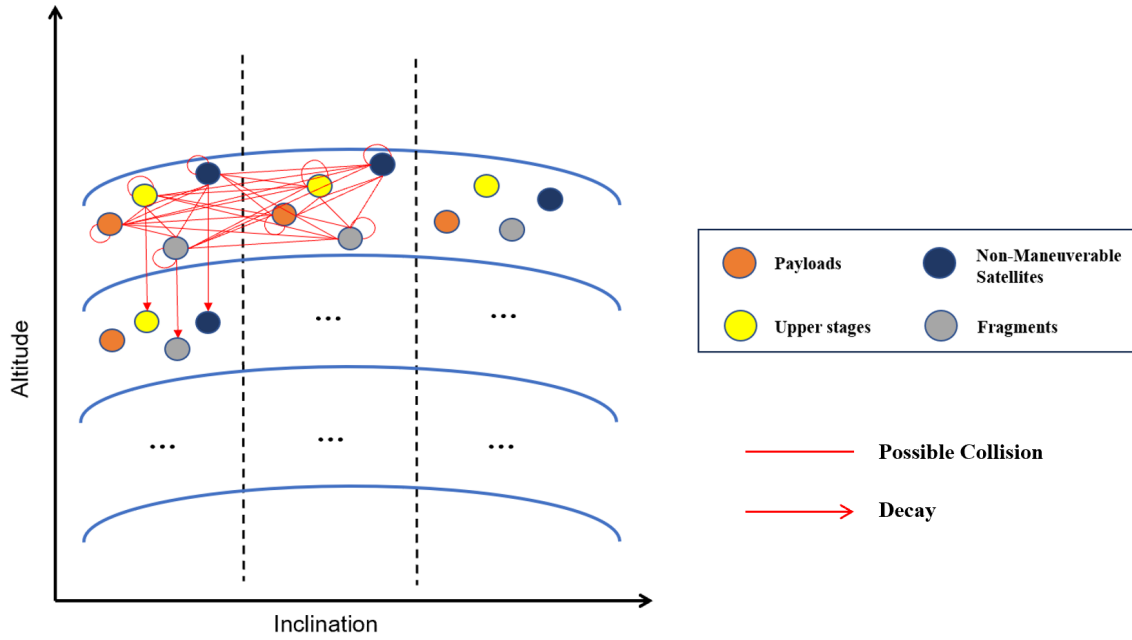


Figure 2: Illustration of the Network Model in physical layer.

NETWORK MODEL

The network model aims to study the relationships among groups of objects in space by studying the topology and dynamics of an equivalent network, where each node is a group of objects and the link is modelling the relationship. Different nodes represent a group of space objects share common properties. In this study, we consider a physical-layer network system consisting of n nodes, and each node is represented by $x_q(t_k)$ that describes the number of the objects in q^{th} node at time t_k , which represents the temporal nature of the network.

Network Dynamics

According to DISCOSWeb database, 4 classes of the space objects are considered: Payloads (P), Upper stages (U), Fragments (F) and Non-Maneuverable satellites (N). Then, each class is further partitioned according to the orbit region, determined by altitude and inclination. For instance, P_{ij} represents the a group of objects labeled with 'Payload' that are located at i^{th} altitude bin and j^{th} inclination bin of the orbit region. Figure 2 shows an illustration of the network model in physical layer. Objects can flow between these nodes, depending on several sink and source phenomena, including collisions, explosions, natural decay due to atmospheric drag, post-mission disposal strategies, operational lifetime duration, and new launches. Note that collisions only occur within orbit shells, which means a lattice structure network is considered in this paper.

In this case the following dynamic equations are considered for node P_{ij} , U_{ij} , N_{ij} and F_{ij}

$$\begin{aligned}
 dP_{ij} &= (-(1 - s_{CAM})[\sum_s \tau(P_{ij}, U_{is}) + \sum_s \tau(P_{ij}, N_{is}) + \sum_s \tau(P_{ij}, F_{is}) + \sum_s \tau(P_{ij}, P_{is})] \\
 &\quad - \kappa \sum_s \tau(P_{ij}, F_{is}) + f_{decay}^{P_{ij}} + f_{explosions}^{P_{ij}} + f_{EoL}^{P_{ij}} + f_{launches}^{P_{ij}})dt \\
 dU_{ij} &= (-[\sum_s \tau(U_{ij}, U_{is}) + \sum_s \tau(U_{ij}, N_{is}) + \sum_s \tau(U_{ij}, F_{is}) + (1 - s_{CAM}) \sum_s \tau(U_{ij}, P_{is})] \\
 &\quad + f_{decay}^{U_{ij}})dt \\
 dN_{ij} &= ([\sum_s \tau(N_{ij}, U_{is}) + \sum_s \tau(N_{ij}, N_{is}) + \sum_s \tau(N_{ij}, F_{is}) + (1 - s_{CAM}) \sum_s \tau(N_{ij}, P_{is})] \\
 &\quad + \kappa \sum_s \tau(P_{ij}, F_{is}) + \gamma P_{ij} + f_{decay}^{N_{ij}} + f_{P2N}^{N_{ij}})dt \\
 dF_{ij} &= (-[\sum_s \tau(F_{ij}, U_{is}) + \sum_s \tau(F_{ij}, N_{is}) + \sum_s \tau(F_{ij}, F_{is}) + (1 - s_{CAM}) \sum_s \tau(F_{ij}, P_{is})] \\
 &\quad + f_{decay}^{F_{ij}} + f_{debris}^{F_{ij}})dt
 \end{aligned} \tag{1}$$

where κ indicates the small collision factor related to the probability of maneuverability being lost due to a collision with non-trackable debris, s_{CAM} indicates the probability of successfully performing collision avoidance maneuvers, and γ indicates the failure rate of post mission disposal. τ indicates the collision rate. $f_{decay}^{P_{ij}}$, $f_{decay}^{U_{ij}}$, $f_{decay}^{N_{ij}}$ and $f_{decay}^{F_{ij}}$ indicate the decay rate of nodes P_{ij} , U_{ij} , N_{ij} and F_{ij} . $f_{P2N}^{N_{ij}}$ indicates the maneuverable satellites flow to non-maneuverable satellites node F_{ij} due to small collisions. The detailed models of the above processes are introduced in the following subsections.

Launch Traffic Model This launch model is based on historical launch data and estimates the future launch rates. Historical data to fit the model are taken from DISCOSWeb. The total number of objects launched in a certain year is given by an exponential logistic curve of the form

$$N = n_0 + \frac{A \cdot e^{d(t-t_0)}}{b + e^{-c(t-t_0)}} \tag{2}$$

Where t is expressed in years and the parameters A , b , c , d , and t_0 control the shape of the curve. These parameters can be selected based on historical trends and predicted future increases in launch traffic. Launched objects are either payloads, upper stages, or mission related objects. The proportion of each is based on the most recent years of launches. For each object class, orbital and physical parameters of historical launches are fit to a Gaussian Mixture Model (GMM), which has the form

$$p(\vec{x}) = \sum_{i=1}^K w_i \phi(\vec{x} | \mu_i, \Sigma_i) \tag{3}$$

where K is the number of GMM components w_i , μ_i , Σ_i are the weight, mean, and covariance associated with the i th GMM component, and ϕ is the standard normal distribution. The associated parameters of each launched object come from sampling this distribution. Separate distributions are fit for the orbital parameters of semimajor axis and inclination, and the physical parameters of mass, area, and length. After establishing real values for these parameters, they are assigned to the relevant node in the graph.

Collision Model The mean collision rate between node i and node j is given by

$$\tau = 4\pi r^2 \cdot \Delta r \cdot \rho_i(r, t) \cdot \rho_j(r, t) \cdot \sigma(i, j) \cdot v^{ref}(r) \quad (4)$$

where σ and v^{ref} are the collision cross-sectional area³ and mean relative collision velocity between the two nodes

$$\begin{cases} \sigma(i, j) = \pi(r_i + r_j)^2 \\ v^{ref}(r) \approx \frac{14\sqrt{2}}{15} \sqrt{\frac{\mu}{r}} \end{cases} \quad (5)$$

The Poisson distributions are used to compute if a collision between objects has to happen. The total collision rate of the entire network is computed by summing, at each time step, the collision rates of every node. The number, the physical parameter distribution and the velocity distribution of the generated fragments can be calculated by NASA's breakup model,¹⁷ while the catastrophic collisions are defined as those with impact kinetic energy to target mass ratio greater than 40 J/g.¹⁸

Explosion Model Similar to the launch model, the model of explosions is based on historical fragmentation data from DISCOSWeb. As defined in ESA's Space Environment Report,¹⁹ the historical events considered are non-system related fragmentations, where the object fragmentation is not due to a systemic design flaw. The number of explosions depends on the launch traffic, with the total number being a proportion of the launched objects. Each launched object added to the model has an associated probability of fragmenting from an explosion that is based on its object class and determined based on recent fragmentations. For upper stages, this probability is X and for payloads Y while mission related objects have 0 probability of exploding.

Objects that are randomly selected as having a fragmentation event will either fragment on the same day they are launched, or some time after it is launched. The probability of fragmenting on the same day as launch is X for upper stages and Y for payloads. Other fragmenting objects have a fragmentation time sampled from a distribution that is fit to previous fragmentation events and depends on the object class. This distribution is a kernel density estimate (KDE) of data from previous non-system related fragmentations.

Decay Model The atmospheric model is confined to satellite with orbit totally below about 500 km. The variation in density due to the space environment is introduced through T which is specified as a function of the solar radio flux $F10.7$ and geomagnetic index A_p . The set of defining equations for the model are given by

$$\begin{aligned} T &= 900 + 2.5(F10.7 - 70) + 1.5A_p \\ m &= 27 - 0.012(h - 200) \\ H &= T/m \\ \rho &= 6 \times 10^{-10} \exp(-(h - 175)/H) \end{aligned} \quad (6)$$

The reduction in the period P due to atmospheric drag is given by

$$dP/dt = -3\pi a \rho (A_e/m) \quad (7)$$

where $A_e = AC_d$. If an object in the lowest orbital shell decays, it is assumed to have completed deorbit, and is removed from the corresponding node.

Multi-layer Nature of the Network

In reality, $x_q(t_k)$ can be vectors of properties and include, for example, also the orbital elements. Each property can follow its own dynamics. If $x_q(t_k)$ is the vector with different properties the network becomes multi-layer, how to study or model relationships across layers is an open problem because layers are not homogeneous. For example, how orbital dynamics affects collision rate is clear, how the number of objects affects the orbital dynamics is not immediately obvious. One would need to express the dependency of the change in orbital elements through the collision model which in turn depends on the number of objects. Therefore, define supra-adjacency matrix is

$$\mathbf{G} = (\mathbf{A}, \mathbf{O}) \quad (8)$$

where $\mathbf{A} = \{\mathbf{A}^{[1]}, \mathbf{A}^{[2]}, \dots, \mathbf{A}^{[M]}\}$ indicates the adjacency matrix in each layer.

$$\mathbf{A}^{[\alpha]} = (V^{[\alpha]}, E^{[\alpha]}) \quad (9)$$

where $V^{[\alpha]}$ indicates the set of nodes in α layer, and $E^{[\alpha]} \subseteq V^{[\alpha]} \times V^{[\alpha]}$ indicates the set of links that connect the pairs of nodes in α layer.

THEORETICAL ANALYSIS OF THE NETWORK

This section first introduces analytical solutions of a simplified network model, which allows us to have a first indication of network's long-term behaviour. Then, some graph theoretical tools are applied to analyze the relationships among nodes.

Analytical Solution

The complexity of the aforementioned network model can be reduced by considering a simplified equation, which allows us to prove the existence of the Kessler Syndrome by analysing the average behaviour of the network. In this case, we assume there is no traffic and no other objects except fragments, only collision and decay processes are considered

$$\dot{x} = c \cdot \tau(x, x) + \epsilon(x) \quad (10)$$

where $\tau(x, x)$ is the collision rate and c is the number of fragments generated from the collision. Decay rate $\epsilon(x)$ is a sink term that used the model to remove the objects from the environment. In this case, a Bernoulli type of differential equation can be written as

$$\dot{x} = qx^2 + px \quad (11)$$

where $q = \frac{c \cdot \tau(x, x)}{x^2}$ and $p = \frac{\epsilon(x)}{x}$. The corresponding analytical solution is

$$x = \frac{e^{-pt}}{C - \int qe^{-pt} dt} \quad (12)$$

For $C = \int qe^{-pt} dt$ the solution x has a vertical asymptote if $q > p$, the corresponding t_c indicates the predicted time of the occurrence of the Kessler syndrome.

$$t_c = -\frac{1}{p} \ln \left(1 - \frac{p}{q} C\right) \quad (13)$$

Centrality Measures

Several methods exist to investigate the network properties from its topology. Some of these properties focus on the interplay between topology and dynamics, while others attempt to characterize how important each node is. By using the matrix representation of the network, we can calculate network properties such as degree and other centralities. Consider the following discrete map of Eq.(1)

$$\mathbf{X}_{k+1} = \mathbf{X}_k + d\mathbf{X}_k \quad (14)$$

Then transform the dynamics of the network into a quasi-linear model along the trajectories of the dynamics, the compact form of the system is then

$$\mathbf{X}_{k+1} \approx \mathbf{A}_k \mathbf{X}_k + \mathbf{g}_k(t) \quad (15)$$

where relationships across the nodes and node-self dynamics are hidden in the coefficient matrix \mathbf{A}_k , and time-dependent terms are hidden in the $\mathbf{g}_k(t)$. The element a_{ij} represents the change of node x_i due to the interaction with node x_j per unit x_j

$$a_{ij} = \begin{cases} 1 + N_{ij}^i(x_i, x_j)/x_j, & i = j \\ N_{ij}^i(x_i, x_j)/x_j, & i \neq j \end{cases} \quad (16)$$

Therefore, the importance of the nodes and links can be evaluated by analyzing the centrality of the \mathbf{A}_k . The simplest centrality measure is the degree centrality, which measures how many neighboring nodes each node has²⁰

$$deg(i) = \sum_{j=1}^n a_{ij} \quad (17)$$

The eigenvalues of \mathbf{A}_k associated with graphs are related to graph connectivity and if the matrix is stochastic, and the Markov chain system converges, then the eigenvectors represent potential final states to become the "true" final state.

Percolation theory

Percolation theory is a set of theories in the field of mathematics and statistical physics to characterize the structure, functionality, and resilience of network systems. Reference [16] firstly proposed percolation model, which is considered to be the pioneers in the study of percolation theory. The idea of percolation theory is to study the robustness of a network, which aims to look for solutions for disaster recovery under extreme cases. Assuming a network consists of 500 nodes, where a 500×500 matrix can be used to represent the links among the nodes. Let p be a threshold to indicate the occurrence of the collision, therefore, given a random number of a uniform distribution ν , we have $\nu > p$ for a collision link. Defining the size of the cluster as the number of connected links, Figure 3 shows the clusters when $p = 0.5$, $p = 0.59$ and $p = 0.6$. Due to the symmetric nature of the matrix, the distribution of connected links is also symmetric. Simulation results suggest that a threshold lying between $p = 0.59$ and $p = 0.6$ appears to result in only one cluster existing in the network, meaning that the collision events 'percolate' throughout the entire network. Furthermore, given the size of the largest cluster S_{max} and number of the nodes n , the percolation probability is defined as S_{max}/n^2 . Figure 4 shows the changes in percolation probability with respect to the probability of collision p , indicating a phase transition occurs at $p \approx 0.595$.

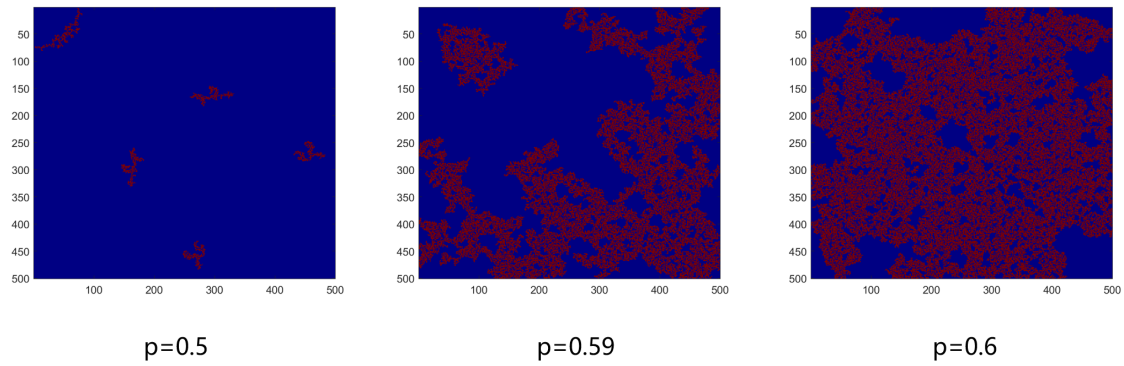


Figure 3: Test case of the percolation theory.

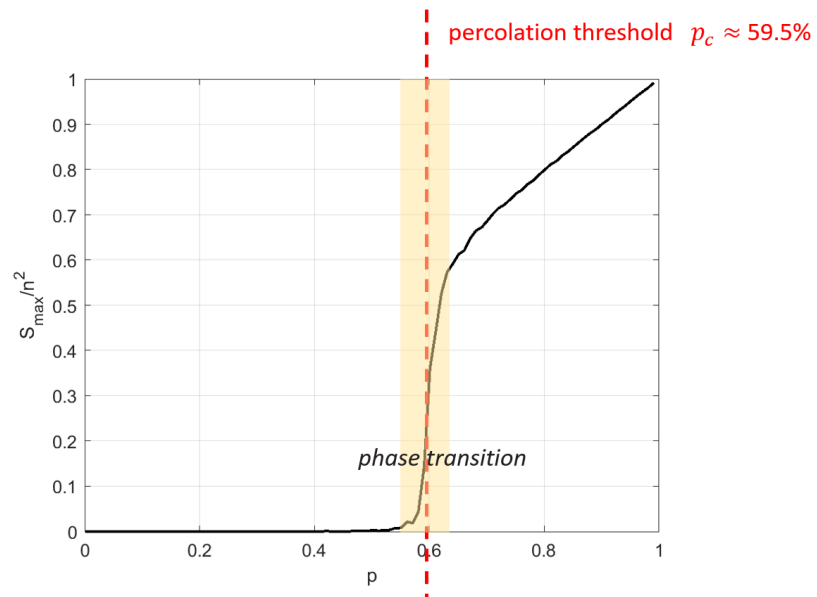


Figure 4: Percolation probability changes with respect to the probability of collision p .

SIMULATION RESULTS

Before analyzing the topology of the network itself, the predictions results of the MTN should be verified. Therefore, in this section, the comparison against the space environment evolution model proposed in Reference [21] is implemented. Two scenarios are considered for the comparison: 1) Baseline, which excludes any consideration of upcoming launches. 2) A Large Constellation (LC) consisting of 30,000 medium satellites at 600-km orbit, while only the satellites in the LC are replenished over time, other constellations and individual satellites are not replaced as the deorbit, fail, or fragment.

Initial conditions are considered as same as mentioned in the Reference [21]: κ is small collision factor that indicates the collisions between payloads and small fragments between 1 cm and 10 cm, and is set to 5.3. s_{CAM} is the probability of successfully performing collision avoidance maneuvers and is set to 99.9 %. 5 years is selected as a representative value for the life time of the satellites, and failure rate of post mission disposal γ is set to 5 %. Only objects above 10 cm in size are considered. The considered altitude spans from 200 km to 2000 km, with each orbital shell, defined every 25 km, and inclination spans from 0° to 180° . Each Fragment node (F) is further partitioned into three groups according to the size of debris: 1 to 3 m diameter debris are grouped as large debris, 0.3 to 1 m diameter debris are grouped as medium debris and 0.1 to 0.3 m diameter debris are grouped as small debris.

Validation of the network model

Test Case 1: Baseline The simulation covers the period from 2021 to 2121, with a yearly time step. Figure 5 shows the evolution of the baseline scenario over 100 years. The total count of fragments larger than 10 cm grows from 10^4 to 10^5 in the next 100 years. Over the course of around 30 years, the number of maneuverable satellites declines from 10^3 to zero due to both the 5-year lifespan model and small collisions. Meanwhile, the number of non-maneuverable satellites initially increases due to the small collisions and the failures of maneuverable satellites. However, the increase rate is reduced as the number of maneuverable satellites decreases, and the subsequent decay process ultimately leads to a decrease in the number of non-maneuverable satellites. In comparison to the spatial density of fragments, the lower spatial density of inactive objects results in a reduced collision rate between inactive objects themselves. Furthermore, this collision rate continues to decrease as the number of inactive objects diminishes. Notably, the baseline case simulation does not predict the occurrence of Kessler Syndrome after 100 years. Compared with the simulation results of baseline scenario in reference,²¹ as shown in Figure 6, the evolution results based on the methods proposed in this paper appear in the same order of magnitude over on 100 years. Figure 7 and Figure 8 show the distribution of the fragments in different orbital regions in year 2021 and year 2121 respectively, which indicates that the orbital region of altitude ~ 1000 km and inclination $\sim 80^\circ$ will become rather risky in year 2121 due to the large amount of the fragments.

Since no launch traffic is considered in the baseline case, upper stages are only consumed by decay and collisions. Figure 9 shows the cumulative count of various collision types over 100 years: collision between inactive objects (intact-intact), collision between an inactive object and a fragment (intact-frag), and collision between fragments (frag-frag). On average, our predictions suggest 34 collisions will occur within the next 100 years. During the initial two decades, most collisions involve 'intact-frag', as many of the collisions between non-maneuverable satellites and fragments have kinetic impact energy greater than 40 J/g. Consequently, the spatial density of fragments increases while that of non-maneuverable satellites decreases. The increase of fragments

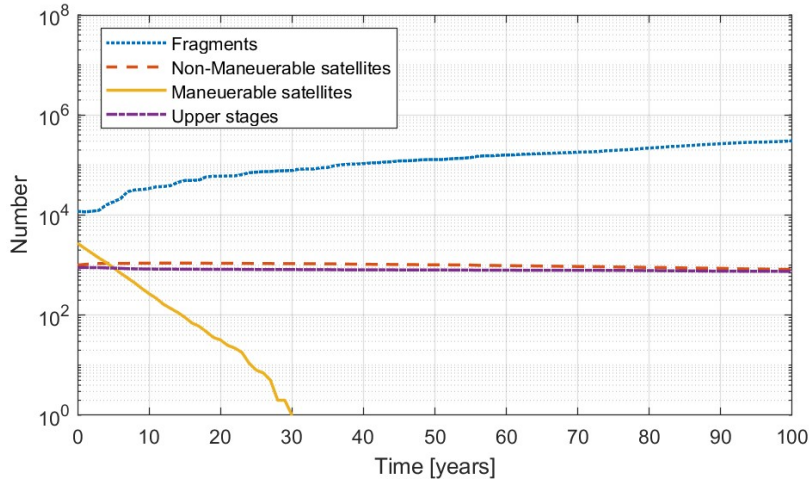


Figure 5: Baseline Case Evolution (this paper).

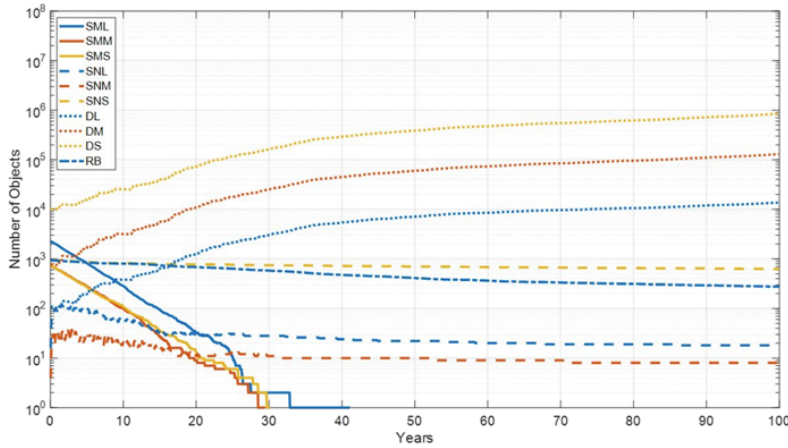


Figure 6: Baseline Case Evolution (reference²¹).

appears to result in an exponential rise in 'intact-frag' and 'frag-frag' collisions. Ultimately, 'frag-frag' type collisions dominate the collision events after 100 years.

Test Case2: 30,000 medium satellites at 600-km orbit In this scenario, more maneuverable satellites will be consumed by un-trackble debris, therefore, leads to a increase spatial density of non-maneuverable satellites. Fragmentation of LC satellites that lose maneuverability due to failures or small object collisions cause the increase of non-maneuverable satellites. As a consequence, the number of fragments appears to grow exponentially, which tends to trigger Kessler Syndrome within 30 years. Figure 11 shows the evolution of the test case 1 over 100 years.

During the first couple of years, the increase of non-maneuverable satellites caused by small collisions is higher than the decrease of non-maneuverable satellites caused by 'intact-frag' collisions. Once the the number of large fragments (larger than 10 cm) generated from 'intact-frag' collisions becomes large enough, the growth of the non-maneuverable satellites reaches an extreme point, resulting in a subsequent decrease in the number of non-maneuverable satellites. Simulation results

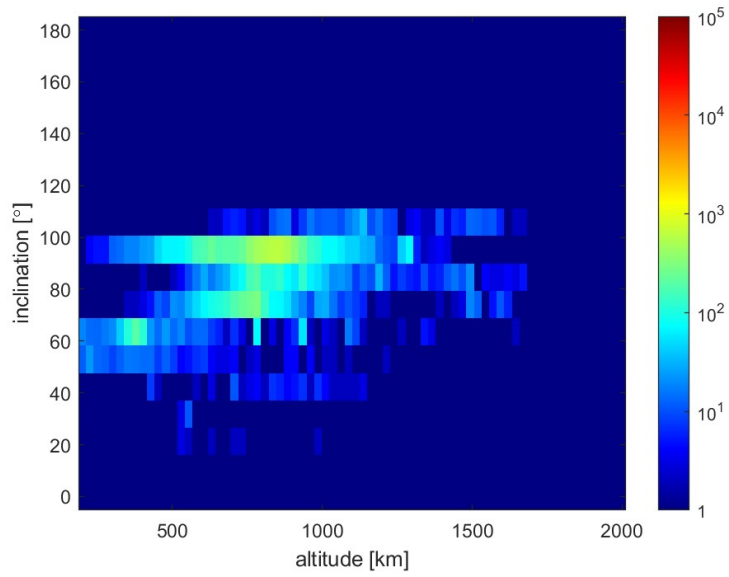


Figure 7: Number of fragments in different orbit region in year of 2021.

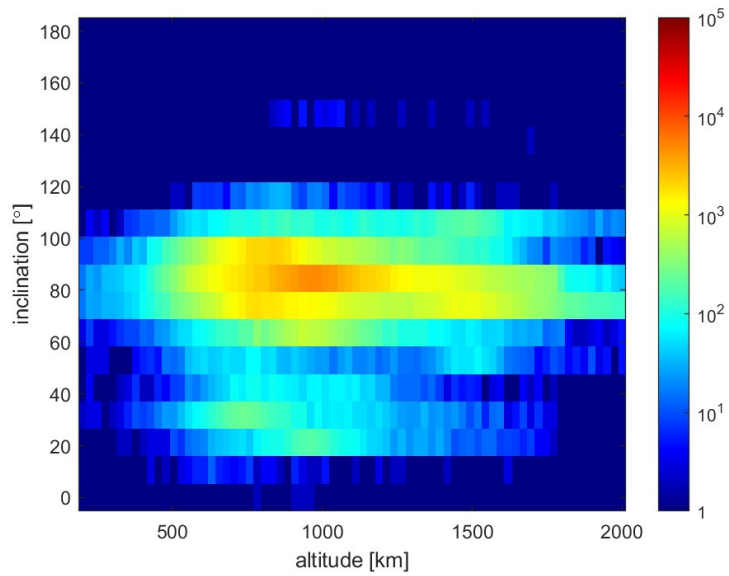


Figure 8: Number of fragments in different orbit region in year of 2121.

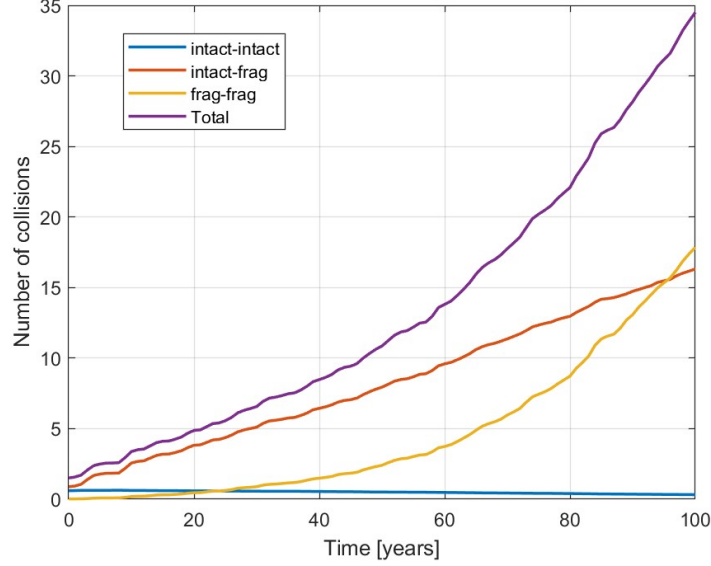


Figure 9: Baseline Case Evolution: Cumulative numbers of collisions as functions of time.

illustrate the importance of post-mission disposal for upper stages and satellites to limit the growth of future on-orbit collisions.

Theoretical analysis of the network

Theoretical analysis is implemented based on a simplified two-node network model. Let x represent the number of inactive objects and y represent the number of active objects. The discrete map of the simplified dynamical model is given by

$$\begin{aligned} x_{k+1} &= x_k + \tau(x_k, y_k) + \eta(x_k, x_k) + \epsilon(x_k) \\ y_{k+1} &= y_k + \sigma(x_k, y_k) + \alpha(y_k, y_k) + \Lambda(t_k) \end{aligned} \quad (18)$$

where $\Lambda(t_k)$ is the launch traffic and $\epsilon(t_k, x_k)$ is the explosion rate that depends on the number of objects that can explode and is also an explicit function of time if one assumes, for example, a Poisson distribution to compute the probability of an object x to explode. Considering the compact form Eq.(15) and the definition of the coefficient matrix \mathbf{A}_k , Eq.(18) can be written as

$$\begin{aligned} x_{k+1} &= a_{11}(x_k)x_k + a_{12}(x_k, y_k)y_k + \epsilon_k(t_k, x_k) \\ y_{k+1} &= a_{22}(y_k)y_k + a_{21}(x_k, y_k)x_k + \Lambda_k(t_k) \end{aligned} \quad (19)$$

where

$$a_{11} = 1 + \frac{\eta(x_k, x_k)}{x_k}, a_{12} = \frac{\tau(x_k, y_k)}{y_k}, a_{21} = \frac{\sigma(x_k, y_k)}{x_k}, a_{22} = 1 + \frac{\alpha(y_k, y_k)}{y_k} \quad (20)$$

the expression of the time dependent term \mathbf{g}_k is

$$\mathbf{g}_k(t_k, x_k, y_k) = [\epsilon(t_k, x_k), \Lambda(t_k)]^T \quad (21)$$

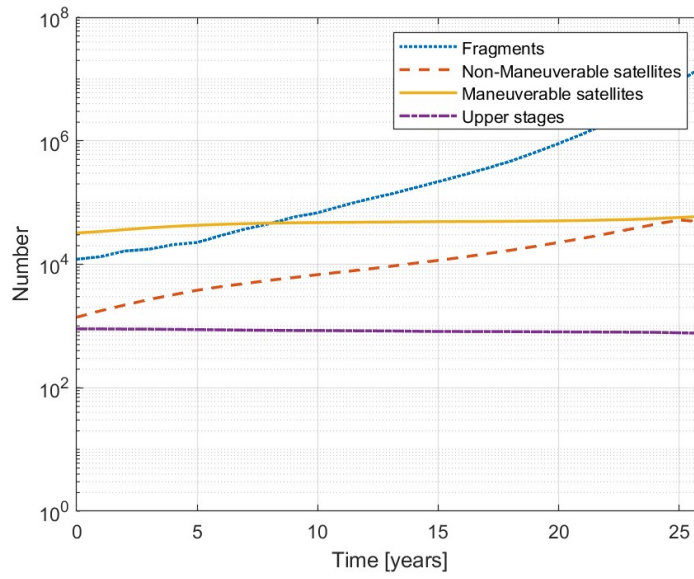


Figure 10: 30,000 medium satellites at 600-km orbit.

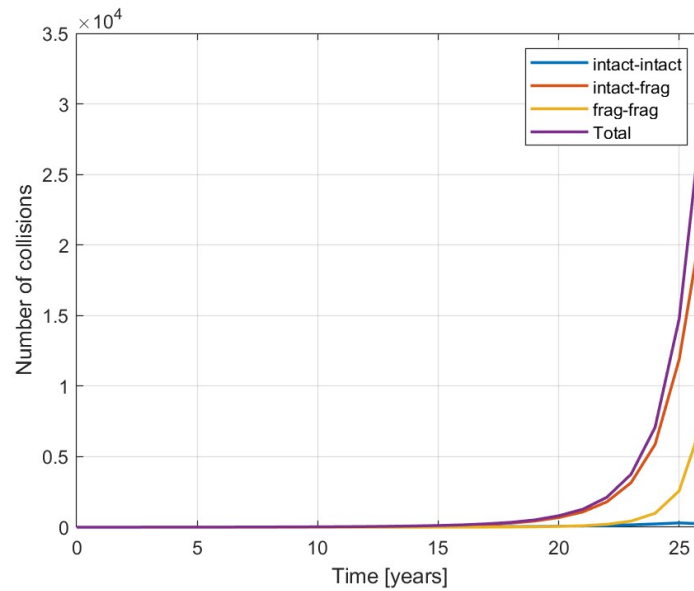


Figure 11: 30,000 medium satellites at 600-km orbit: Cumulative numbers of collisions as functions of time.

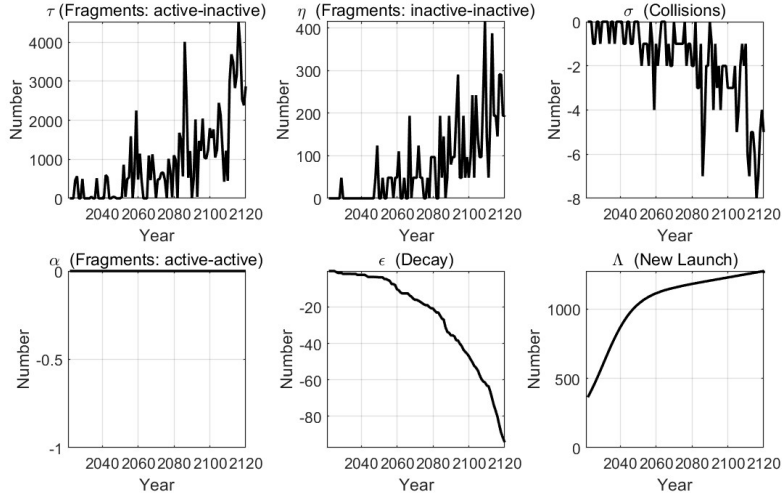


Figure 12: Evolution of different terms in node dynamic equations.

Considering the population in the DISCOSWeb database and assuming that active-active collisions do not occur, the simulation covers the period from 2021 to 2121. At each time step, coefficient matrix \mathbf{A}_k can be calculated according to Eq.(20). Therefore, Figure 12 shows the evolution of $\tau, \eta, \sigma, \alpha, \epsilon, \Lambda$ over 100 years, and Figure 13 shows the evolution of the coefficient matrix \mathbf{A}_k . Furthermore, Figure 14 shows the degree of nodes x and y at each time step. Simulation results suggest that the degree of node x is always greater than or equal to the degree of node y , which means that the group of inactive objects is more important than the group of active objects over 100 years.

CONCLUSIONS

In this paper, the concept of Multi-Layer Temporal Network Model (MTN) for investigating space environment is proposed. We model the space environment base on a network model and investigate the network dynamics. Simulation results of network-based space environment model appear in agreement with previous results. Meanwhile, theoretical analysis of the network topology is performed based on a simplified two-node model, which shows the basic functionalities of a network-based space environment model. In the future, we plan to study more topologies of the network and to analyze the role of different control strategies for stabilizing the space environment evolution and reducing the risk of the Kessler Syndrome.

ACKNOWLEDGMENT

This work was supported through the Horizon 2020 MSCA ETN Stardust-R (grant agreement number: 813644). ESA OSIP Multi-layer Network Model of the Space Environment, contract 4000129448/20/NL/MH, Project officer: Francesca Letizia.

REFERENCES

- [1] A. M. Bradley and L. M. Wein, “Space debris: Assessing risk and responsibility,” *Advances in Space Research*, Vol. 43, No. 9, 2009, pp. 1372–1390.

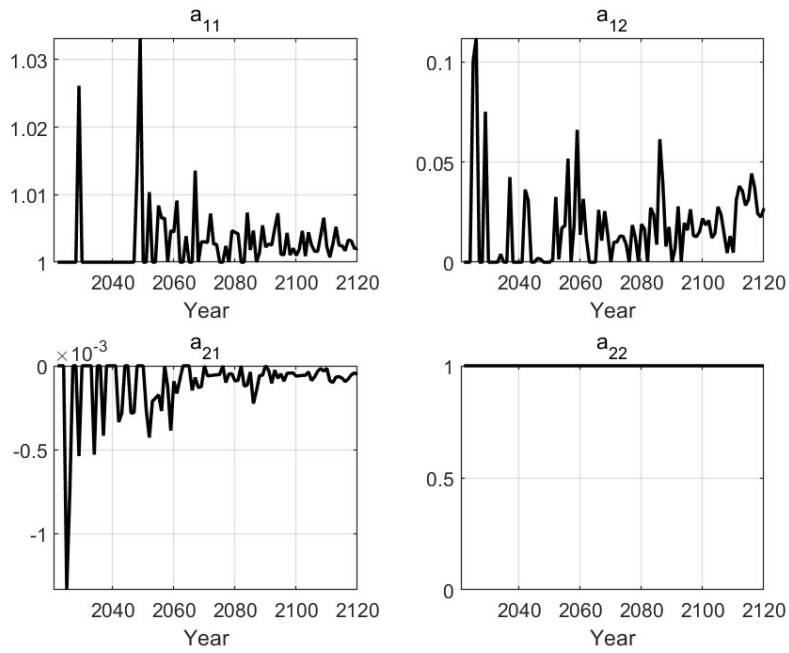


Figure 13: Evolution of the coefficient matrix \mathbf{A}_k over 100 years.

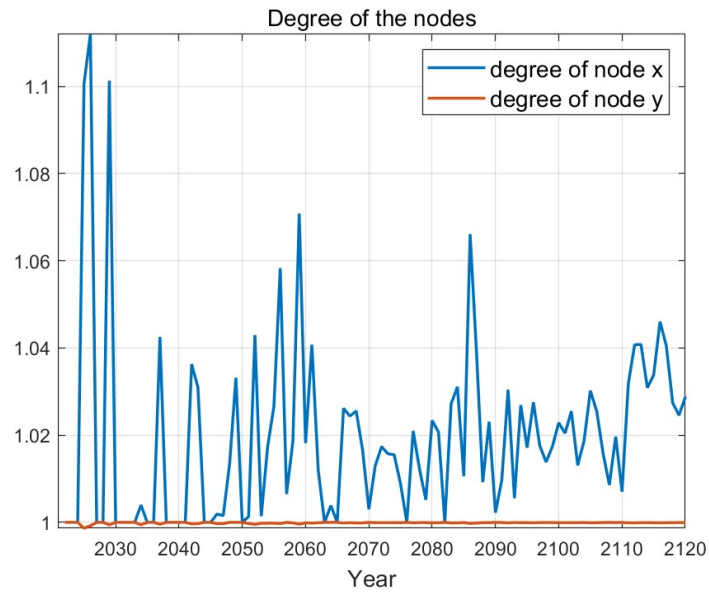


Figure 14: Degree of the nodes.

- [2] J. C. Liou and N. L. Johnson, "A sensitivity study of the effectiveness of active debris removal in LEO," *Acta Astronautica*, Vol. 64, No. 2-3, 2009, pp. 236–243.
- [3] D. J. Kessler and B. G. Cour-Palais, "Collision frequency of artificial satellites: The creation of a debris belt," *Journal of Geophysical Research Space Physics*, Vol. 83, No. A6, 1978, pp. 2637–2646.
- [4] N. Adilov, P. J. Alexander, and B. M. Cunningham, "An economic "Kessler Syndrome": A dynamic model of earth orbit debris," *Economics Letters*, Vol. 166, No. MAY, 2018, pp. 79–82.
- [5] T. J. Muelhaupt, M. E. Sorge, J. Morin, and R. S. Wilson, "Space traffic management in the new space era," *Journal of Space Safety Engineering*, Vol. 6, No. 2, 2019, pp. 80–87.
- [6] J.-C. Liou, D. Hall, P. Krisko, and J. Opiela, "LEGEND—A three-dimensional LEO-to-GEO debris evolutionary model," *Advances in Space Research*, Vol. 34, No. 5, 2004, pp. 981–986.
- [7] B. B. Virgili, "DELTA debris environment long-term analysis," *Proceedings of the 6th International Conference on Astrodynamics Tools and Techniques (ICATT)*, 2016.
- [8] J.-C. Liou, D. J. Kessler, M. Matney, and G. Stansbery, "A new approach to evaluate collision probabilities among asteroids, comets, and kuiper belt objects," *Lunar and Planetary Science Conference*, 2003, p. 1828.
- [9] J. Dolado-Perez, R. Di Constanzo, and B. Revelin, "Introducing MEDEE—A new orbital debris evolutionary model," *Proceeding of the 6th European Conference on Space Debris*, 2013.
- [10] X.-w. Wang and J. Liu, "An introduction to a new space debris evolution model: SOLEM," *Advances in Astronomy*, Vol. 2019, 2019, pp. 1–11.
- [11] R. Walker, P. Stokes, J. Wilkinson, and G. Swinerd, "Enhancement and validation of the IDES orbital debris environment model," *Space Debris*, Vol. 1, 1999, pp. 1–19.
- [12] R. Lucken and D. Giolito, "Collision risk prediction for constellation design," *Acta Astronautica*, Vol. 161, 2019, pp. 492–501.
- [13] J. Zhang, Y. Yuan, K. Yang, and L. Li, "Long-Term Evolution of the Space Environment Considering Constellation Launches and Debris Disposal," *IEEE Transactions on Aerospace and Electronic Systems*, 2023, pp. 1–17, 10.1109/TAES.2023.3274097.
- [14] A. Boley and M. Byers, "Satellite mega-constellations create risks in Low Earth Orbit, the atmosphere and on Earth," *Nature Publishing Group*, 2021.
- [15] V. Latora, V. Nicosia, and G. Russo, *Centrality Measures*, p. 31–68. Cambridge University Press, 2017, 10.1017/9781316216002.004.
- [16] S. R. Broadbent and J. M. Hammersley, "Percolation processes: I. Crystals and mazes," *Mathematical proceedings of the Cambridge philosophical society*, Vol. 53, Cambridge University Press, 1957, pp. 629–641.
- [17] N. L. Johnson, P. H. Krisko, J.-C. Liou, and P. D. Anz-Meador, "NASA's new breakup model of EVOLVE 4.0," *Advances in Space Research*, Vol. 28, No. 9, 2001, pp. 1377–1384.
- [18] L. N., Johnson, , , H. P., Krisko, , , J.-C., Liou, , , and D. P., "NASA's new breakup model of evolve 4.0," *Advances in Space Research*, 2001.
- [19] S. Lemmens and F. Letizia, "ESA's Annual Space Environment Report," LOG GEN-DB-LOG-00288-OPS-SD, European Space Agency, June 2023.
- [20] G. Acciarini and M. Vasile, "A Multi-Layer Temporal Network Model of the Space Environment," *71st International Astronautical Congress (IAC) - The CyberSpace Edition*, 2020.
- [21] M. Sturza and G. S. Carretero, "Design Trades for Environmentally Friendly Broadband LEO Satellite Systems," 2021.